JOURNAL OF AGRICULTURAL AND FOOD CHEMISTRY
ARTICLE

J. Agric. Food Chem. 2010, 58, 12847–12857 12847
DOI:10.1021/jf102764e

# Morphology and Water Barrier Properties of Nanobiocomposites of κ/ι-Hybrid Carrageenan and Cellulose Nanowhiskers

Maria Dolores Sánchez-García,[†] Loic Hilliou,[§,#] and José María Lagarón*,[†]

[†]Novel Materials and Nanotechnology Group, IATA, CSIC, Apartado Correos 73, 46100 Burjassot, Spain, [§]Institute for Polymers and Composites/I3N, University of Minho, Campus de Azurém, 4800-058 Guimarães, Portugal, and [#]REQUIMTE-Faculty of Engineering, University of Porto, Rua Dr. Roberto Frias s/n, 4200-465 Porto, Portugal

The current study presents the development and characterization of novel carrageenan nanobiocomposites showing enhanced water barrier due to incorporation of cellulose nanowhiskers (CNW). CNW, prepared by acid hydrolysis of highly purified α cellulose microfibers, were seen to have a length of around 25−50 nm and a cross section of ca. 5 nm when dispersed in the matrix. The nanobiocomposites were prepared by incorporating 1, 3, and 5 wt % of the CNW into a carrageenan matrix using a solution casting method. Morphological data (TEM and optical microscopy) of the nanocomposites containing CNW were compared with the morphology of the corresponding biocomposites containing the original cellulose microfibers and the differences discussed. Thermal stability by TGA, water vapor permeability, and percent water uptake were also determined. The main conclusion arising from the analysis of the results is that the nanobiocomposites containing 3 wt % of CNW exhibited the lowest reduction in water vapor permeability, that is, ca. 71%, and that this reduction was largely attributed to a filler-induced water solubility reduction. This fully biobased nanoreinforced carrageenan can open new opportunities for the application of this biopolymer in food-packaging and -coating applications.

**KEYWORDS: Carrageenan; food packaging; food coating; biocomposites; cellulose**

## INTRODUCTION

Biopolymer films have been the focus of worldwide attention for the past few decades because they offer favorable environmental advantages in terms of biodegradability compared to conventional synthetic polymeric films. Edible and biodegradable natural polymer films offer alternative packagings and coatings with lower environmental costs. The search for new renewable resources for the production of edible and biodegradable materials has steadily increased in recent years. In particular, nonconventional sources of carbohydrates have been extensively studied. There are various unique carbohydrates that are found in marine organisms that represent a largely unexplored source of valuable materials. These nonconventional and underexploited renewable materials can be used as an interesting alternative to produce edible films and coatings (*4*).

The biopolymers studied in this work to produce edible films and coatings were κ/ι-hybrid carrageenan extracted from *Mastocarpus stellatus*, an underexploited red algae present in the Portuguese marine coast (*1*−*4*). Carrageenans are water-soluble polymers with a linear chain of partially sulfated galactans, which present high potentiality as film-forming materials. Carrageenans are structural polysaccharides from red seaweed and have been used extensively in foods, cosmetics, and pharmaceuticals (*5*). Carrageenan biopolymer extracted from *M. stellatus* seaweeds was shown to be a κ/ι-hybrid carrageenan with gel properties comparable to those of commercial κ-carrageenan gel formers. The use of carrageenan as edible films and coatings already covers various fields of the food industry such as application on fresh and frozen meat, poultry, and fish to prevent superficial dehydration (*6*), ham or sausage casings (*7*), granulation-coated powders, dry solids foods, oily foods (*8*), etc., and also the manufacture of soft capsules (*9*, *10*) and especially nongelatin capsules (*11*). Polysaccharide and protein film materials are characterized by high moisture permeability, low oxygen and lipid permeability at lower relative humidities, and compromised barrier and mechanical properties at high relative humidities (*12*).

To tailor the properties and improve the water resistance of these biopolymers, it is often desirable to blend them with more water-resistant biopolymers or with nanoadditives. In the case of the addition of nanoclays, the nanocomposite films have been seen to substantially reduce water-vapor permeability, solving one of the long-standing problems in the production of biopolymer films and coatings (*13*).

More recently, cellulose nanowhiskers (CNW), also termed cellulose nanocrystals, are increasingly used as load-bearing constituents in developing new and inexpensive biodegradable materials due to their high aspect ratio, good mechanical properties (*14*), and fully degradable and renewable character.

*Author to whom correspondence should be addressed (e-mail lagaron@iata.csic.es).



Published on Web 11/12/2010

As compared to other inorganic reinforcing fillers, CNW have many additional advantages, including a positive ecological footprint, wide variety of fillers available throughout the world, low density, low energy consumption in manufacturing, ease of recycling by combustion, high sound attenuation, and comparatively easy processability due to their nonabrasive nature (*15*, *16*).

Cellulose nanowhiskers are prepared by treating native cellulosic products with acid reagents, most typically sulfuric acid, where small amounts of sulfate ester groups are introduced to the surfaces (*17*). This treatment is, however, hydrolytic and thus results in dramatic decreases in both the yield and fibril length attained down to 100−150 nm. The use of cellulose nanowhiskers as nanoreinforcement is a new field in nanotechnology, and as a result there are still many obstacles remaining regarding their use. Their production is time-consuming and is still associated with low yields. They are difficult to use in systems that are not water based due to their strong self-association by hydrogen bonding. Here, the cellulose nanowhiskers are added to the carrageenan, which is water-soluble. Because cellulose nanowhiskers allow a quite stable dispersion in water, composites are generally obtained with matrices that can be dissolved/suspended in water such as latex (*18*−*20*), starch (*21*, *22*), poly(ethylene oxide) (PEO) (*23*, *24*), chitosan (*25*), and soy protein (*26*). A previous study showed for the first time the capacity of this natural nanoreinforcing element to develop nanobiocomposites of solvent cast PLA by various methods, which resulted in enhanced barrier properties to gases and vapors (*31*).

However, very little is known about the development and characterization of carrageenan nanocomposites. Daniel-Da-Silva et al. reported the use of *ι*-carrageenan polysaccharide for the production of macroporous composites containing nanosized hydroxyapatite, with application in bone tissue engineering (*27*). Gan et al. developed a new injectable biomaterial, carrageenan/nanohydroxyapatite/collagen, for bone surgery (*28*). In a previous work, Sanchez-Garcia et al. reported the development and barrier properties of new nanocomposites of carrageenan based on nanoclays (*13*). However, to the best of our knowledge, the addition of cellulose nanowhiskers to carrageenan and the study of the resulting barrier properties of these novel nanobiocomposites have not been reported before.

Thus, the objective of this work is to develop new fully renewable and biodegradable edible films for food-packaging applications with better barrier properties, especially better water resistance. A top-down nanotechnology approach is used to reach this objective, which consists of the incorporation via solution casting of plant -derived cellulose nanowhiskers previously hydrolyzed from the corresponding microfibers.

## EXPERIMENTAL PROCEDURES

**Materials.** Details about the recovery of *κ*/*ι*-hybrid carrageenan biopolymers from *M. stellatus* seaweeds can be found elsewhere (*1*, *2*, *29*). The polysaccharide used in the present study was obtained through a hot extraction process performed during 2 h at 95 °C and a pH of 8 on alkali-treated *M. stellatus* seaweeds. The resulting powder was then purified by mixing 1 g of isolated product with 50 mL of hot distilled water during 1 h and subsequent centrifugation performed at sequence cycles at $10^4$ rpm (13.7 g) and 40 °C during 40 min. The supernatant was finally recovered and used for film forming by casting.

A highly purified α-cellulose microfiber grade from CreaFill Fibers Corp. (USA), having an average fiber length of 60 $\mu$m and an average fiber width of 20 $\mu$m, was used. According to the manufacturer's specifications, these fibers had an α-cellulose content in excess of 99.5%.

Sulfuric acid (95−97%) from Sigma Aldrich, Germany, was used during the CNW production. Sodium hydroxide from Fluka was also used during neutralization of the CNW. Glycerol was used as plasticizer and was supplied by Panreac Quimica S.A. (Spain).

**Preparation of Nanocomposites.** *CNW Production*. Highly purified α-cellulose microfibers, 10 g/100 mL, were hydrolyzed in 9.1 mol/L sulfuric acid at 44 °C for 130 min. The excess of sulfuric acid was removed by repeated cycles of centrifugation, 10 min at 13000 rpm (20.4*g*). The supernatant was removed from the sediment and was replaced by deionized water. The centrifugation continued until the supernatant became turbid, which suggested that the nanowhiskers became largely released into the solution in accordance with a previous work (*30*). After centrifugation, the suspension containing cellulose nanowhiskers had a pH of 3.5, and the solution was drop by drop neutralized with sodium hydroxide to pH 7 and subjected to dialysis, following a procedure described elsewhere (*33*). The nanofiller was used suspended in water to make the various nanobioblends to avoid potential agglomeration during drying.

*CNW Dispersion and Film Preparation*. Solution-cast film samples of carrageenan containing 1, 3, and 5 wt % of CNW were prepared, using water as a solvent. CNW solutions were mixed in a homogenizer (Ultraturrax T25 basic, Ika-Werke, Germany) for 2 min and were then stirred with the carrageenan at ambient temperature during 30 min and, subsequently, cast onto Petri dishes to generate films of around 50 $\mu$m thickness after solvent evaporation at room temperature conditions. In the case of carrageenan films with glycerol, 10 wt % of glycerol was added to the solution before casting. Similar blends were obtained with 1, 3, and 5 wt % contents of the original cellulose microfibers for comparative purposes.

**Optical Light Polarized Microscopy.** Polarized light microscopy (PLM) examinations using an Eclipse E800-Nikon with a capture camera DXM1200F-Nikon were carried out on both sides of the cast samples.

**Transmission Electron Microscopy (TEM) Measurements.** TEM was performed using a JEOL 1010 equipped with a digital Bioscan (Gatan) image acquisition system. TEM observations were very difficult to perform due to water absorption and difficult handling of the films. However, some pictures were taken on microdrops of the film-forming solutions cast directly onto the TEM observation grids. The solutions were stained before casting by adding a 2 wt % solution of uranyl acetate for 3 min. The pure cellulose nanowhiskers were also observed by direct casting of water suspensions over the TEM grids followed by solvent evaporation.

**Thermogravimetric Analysis (TGA) Measurements.** The thermal stability of both freeze-dried CNW and cellulose microfibers and of the nanocomposites was investigated using a TGA Q500 from TA Instruments USA. The samples were heated from room temperature to 600 °C at a heating rate of 10 °C/min and a nitrogen flow of 100 mL/min.

**Gravimetric Measurements.** Direct water vapor permeability was determined from the slope of the weight gain versus time curves at 24 °C. The films were sandwiched between the aluminum top (open O-ring) and bottom parts of a specifically designed permeability cell with screws containing silica gel to generate 0% relative humidity (RH). A Viton rubber O-ring was placed between the film and the bottom part of the cell to enhance sealability. Then, the cells were placed in the desired environment, namely, a desiccator conditioned at 75% RH generated by a saturated salt solution, and the solvent weight gain through the film was monitored as a function of time. Cells with aluminum films were used as control samples to estimate solvent gain through the sealing. Solvent permeation rates were estimated from the steady-state linear permeation slopes. Water weight gain was calculated as the total cell weight gain minus the gain through the sealing. The tests were done in duplicate.

For the percent water uptake, samples were dried in a desiccator at 0% RH until constant weight to obtain the so-called dry weight. They were then allowed to saturate in moisture inside desiccators at 11, 54, and 75% RH and monitored during sorption until constant weight (indicating water uptake). The experiments were done in triplicate and averaged. The water uptake was calculated as the water gain at the desired RH divided by the dry weight and multiplied by 100.

## RESULTS AND DISCUSSION

**Morphological Characterization. Figure 1** shows typical photographs taken in the cast carrageenan film and its nanocomposite containing 5 wt % CNW and its microcomposite containing 5 wt % cellulose microfiber. Samples with CNW showed the best optical properties, the samples with cellulose microfibers being

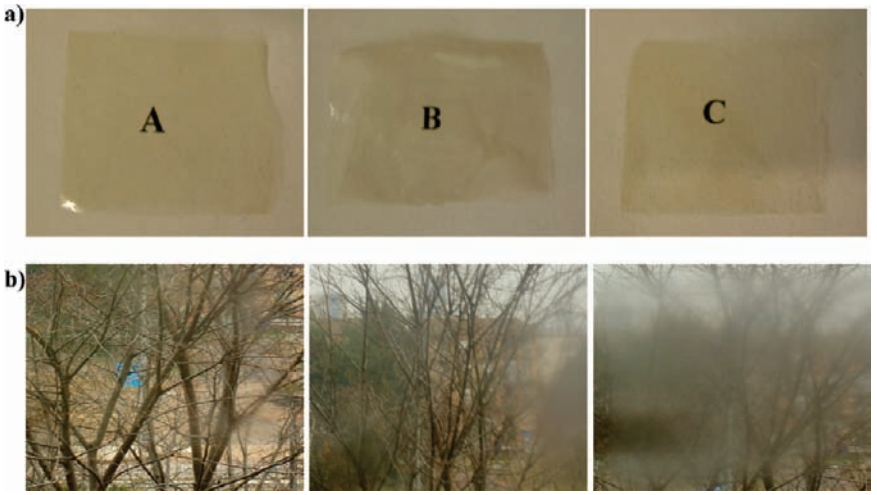


**Figure 1.** Typical photographs of 30 $\mu$m thickness films of (A) carrageenan, (B) carrageenan film containing 5 wt % of CNW, and (C) carrageenan film containing 5 wt % of cellulose microfibers as shown by contact transparency (**a**) and transparency against light (**b**).

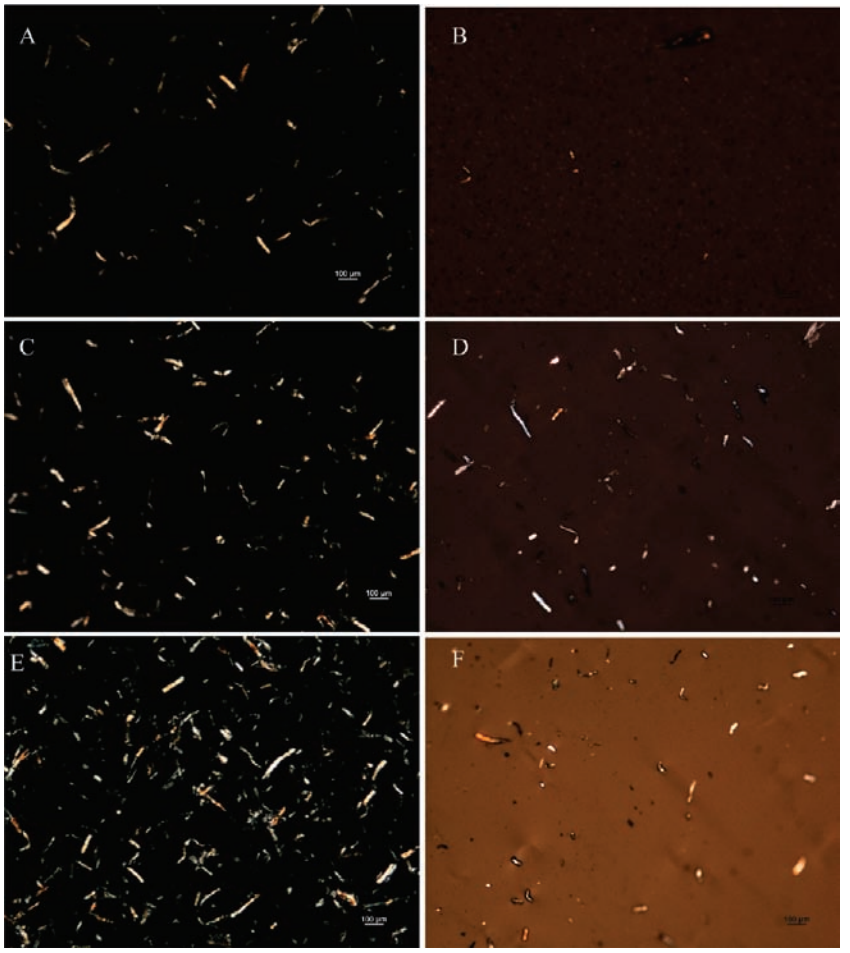


**Figure 2.** Polarized optical micrographs of carrageenan-based films prepared by casting containing (**A**) 1 wt % cellulose microfibers, (**B**) 1 wt % CNW, (**C**) 3 wt % cellulose microfibers, (**D**) 3 wt % CNW, (**E**) 5 wt % cellulose microfibers, and (**F**) 5 wt % CNW. The scale marker is 100 $\mu$m.

less transparent. Both contact transparency (see **Figure 1a**) and transparency against light (see **Figure 1b**) were evaluated. In the contact transparency, the samples appear to exhibit similar behaviors. However, in transparency against light the film containing CNW shows better performance, suggesting that the cellulose nanowhiskers must be well dispersed in contrast to large cellulose microfibers, which scatter light to a significant extent. In any case, unfilled carrageenan films do still show the highest transparency.

Polarized optical microscopy permits one to zoom up the morphology at the micrometer level to observe the carrageenan composites and to potentially assess the efficiency of the hydrolysis and separation processes in the nanocomposites (see **Figure 2**). From this figure, it can be seen that some remaining microfibers can still be detected in the separated CNW fractions. Despite this, the scarce remaining microfiber particles are of course much thinner in comparison with the original microfibers.

Optical microscopy was not often utilized when nanofabrication of cellulose was carried out in the previous literature and, hence, it is difficult to assess whether this is the result of our process or if it is a general effect during the hydrolysis of microfibers. The optimization of the hydrolysis time and the effect of using different acids will be reported elsewhere.

**Figure 2A** indicates that the dimensions of the cellulose microfibers in the biocomposites are not homogeneous but vary from 10 to 30 $\mu$m in the cross section and between 50 and 150 $\mu$m in length across the polymer matrix. For biocomposites with higher filler contents, larger fiber aggregates and agglomeration of the microfibers in the matrix are observed (see **Figure 2E**), as reported by Sanchez-Garcia and Lagaron in previous works (*31*, *32*).

Thus, from this figure, it can be seen that although the hydrolysis was not able to break down completely the fibers, the larger fibers are much thinner and relatively scarce in comparison with the original microfibers also shown for comparison purposes. The films were observed on both sides by optical microscopy and were found to provide similar results, indicating that the observations are not the result of detectable uneven dispersion across the film thickness.

When glycerol was added to the biopolymer, some interesting observations were made. On the one hand, glycerol was seen to form inhomogeneous but rather large segregated domains in the absence of filler (see **Figure 3B**). This is in accordance with previous observations by the authors in the biopolymer amylopeptine plasticized with glycerol (*47*). More interestingly, however, is the observation that in the presence of the microcomposites, the cellulose microfibers do not seem to be homogeneously dispersed and appear to be rather segregated to the matrix fraction (see **Figure 3C−F**). Indeed, when polarized light was used, the microfibers appeared to set aside and to preferentially locate within the matrix fraction. Panels **E** and **F** of **Figure 3** (see arrows) also support the latter observations by suggesting that glycerol domains seem to form boundaries around the fibers. Even more interesting is the fact that when CNW were used, it was much more difficult to spot in the composite the otherwise large glycerol domains, and observation of **Figure 3H** suggests that the glycerol domains become smaller and more homogeneously dispersed across the matrix in the presence of the nanofiller. This could be related to the nanosize of the cellulose whiskers, which makes difficult the aggregation of glycerol in the matrix providing a more homogeneous composite. This observation may also help to explain the completely different water barrier performance of plasticized micro- and nanocomposites (see later).

TEM is a powerful tool for the analysis of cellulose whiskers and nanoparticles dispersion in general. In any case, TEM analysis of the nanocomposite structure was challenging for several reasons: The major problem is the impossibility of microtoming the biocomposite films, because the cuts are usually collected on liquids, which either dissolve the polymer or lead to rolled pieces very difficult to handle and observe. However, by direct casting of polymer solution drops over the TEM grid, relatively good images of the nanobiocomposites were obtained. **Figure 4** shows pictures of the pure carrageenan, pure nanowhiskers, and the corresponding nanobiocomposites. From **Figure 4B** a good dispersion of the nanowhiskers in the matrix becomes apparent; however, increasing the nanofiller content in the matrix (**Figure 4C**) results in an increase in the number of agglomerates, most likely due to the well-reported natural trend of the cellulosic fillers to self-associate via hydrogen bonding as the concentration builds up in composites.

The typical size of the cellulose nanowhiskers as determined by TEM was found to be around 25−50 nm in length and around 5 nm in the cross section within the polymeric matrix. Thus, by comparing the size of the attained CNW with that of the original cellulose microfibers, it becomes evident that a considerable (by ca. 3 orders of magnitude) reduction in fiber size has been accomplished by the acid hydrolysis. These results are in agreement with previous findings by these authors using this type of microfibers (*31*) and also with previous results by other authors using different cellulosic materials (*30*, *31*). Direct TEM observation of the pure cellulose nanowhiskers after solvent evaporation indicates that a very intricate network of aggregated whiskers is formed with cross sections in the thinnest fibers below 10 nm. By drying, the cellulosic material tends to agglomerate and, therefore, it is likely that the presence of the biopolymer molecules in the composites helps to better retain the dispersibility expected to exist in the solution form.

**Thermal Stability.** Thermal degradation of carrageenan and its nanocomposites containing both CNW and the original microfibers was studied by determining the corresponding mass loss during heating by TGA. **Table 1** summarizes the decomposition thermograms (maximum of the weight loss first derivate) for all samples. From **Table 1**, the temperature at which the carrageenan decomposition rate is the highest is 219.78 °C. On the other hand, the weight loss first-derivative maximum for the neat CNW is located at 331.55 °C. This is ca. 32 °C lower than that for the original cellulose microfibers, indicating that the CNW are less thermally stable than the original microfibers, in agreement with previous works (*48*), due to most likely the hydrolysis process that promotes the presence of sulfate groups on the fiber surface. At low contents of CNW (1 and 3 wt %), the decomposition temperature of the biocomposites without glycerol decreases; however, further incorporation of CNW (5 wt %) results in a slightly increased thermal stability.

For the films of carrageenan containing glycerol, the decomposition temperature increased by 4 °C, suggesting that the plasticizer stabilizes the polymer to some extent. In the case of the nanocomposite samples containing glycerol, the decomposition temperature also increased by ca. 8 °C, suggesting that glycerol can also act as a stabilizer for the blend. This increase was arrested for the composites containing CNW in excess of 3 wt %. Pandey et al. reported a decrease in thermal stability with the addition of cellulose nanowhiskers to a PLA matrix(*34*). The authors discussed that there are conflicting reports about the thermal stability of esterified lignocellulosic materials, the behavior of which was seen to depend on the reagents used for modification. Esterification with maleic and succinic anhydrides was also reported to lead to a decrease in thermal stability, whereas treatment with fatty acids, acrylonitrile, methyl methacrylate, did enhance thermal stability (*34*). Chen et al. also showed a reduction in decomposition temperature with the addition of pea hull fiber (PHF)-derived nanowhiskers to pea starch ascribed to the longer interaction with the acid media (*35*). Ayuk et al. reported that an improvement in thermal degradation temperatures, even at high whisker contents, is considered to be an indication for efficient dispersion of the filler (*36*). On the other hand, Li et al. reported that the decomposition temperature of chitosan films containing CNW derived from cotton linter pulp hardly changed with an increase in nanofiller content in the matrix. The latter authors suggested that the addition of CNW retained the thermal stability of the films because of the strong interactions between the whiskers and chitosan (*37*).

Addition of cellulose microfibers to unplasticized carrageenan resulted in a continuous decrease in the decomposition temperature for microfiller loadings of up to 3 wt %. Thus, whereas 1 wt % of CNW dropped the most the thermal stability and further nanofiller loading resulted in increased stability, for the microfibers the maximum drop was for 3 wt % loading. On the other hand,

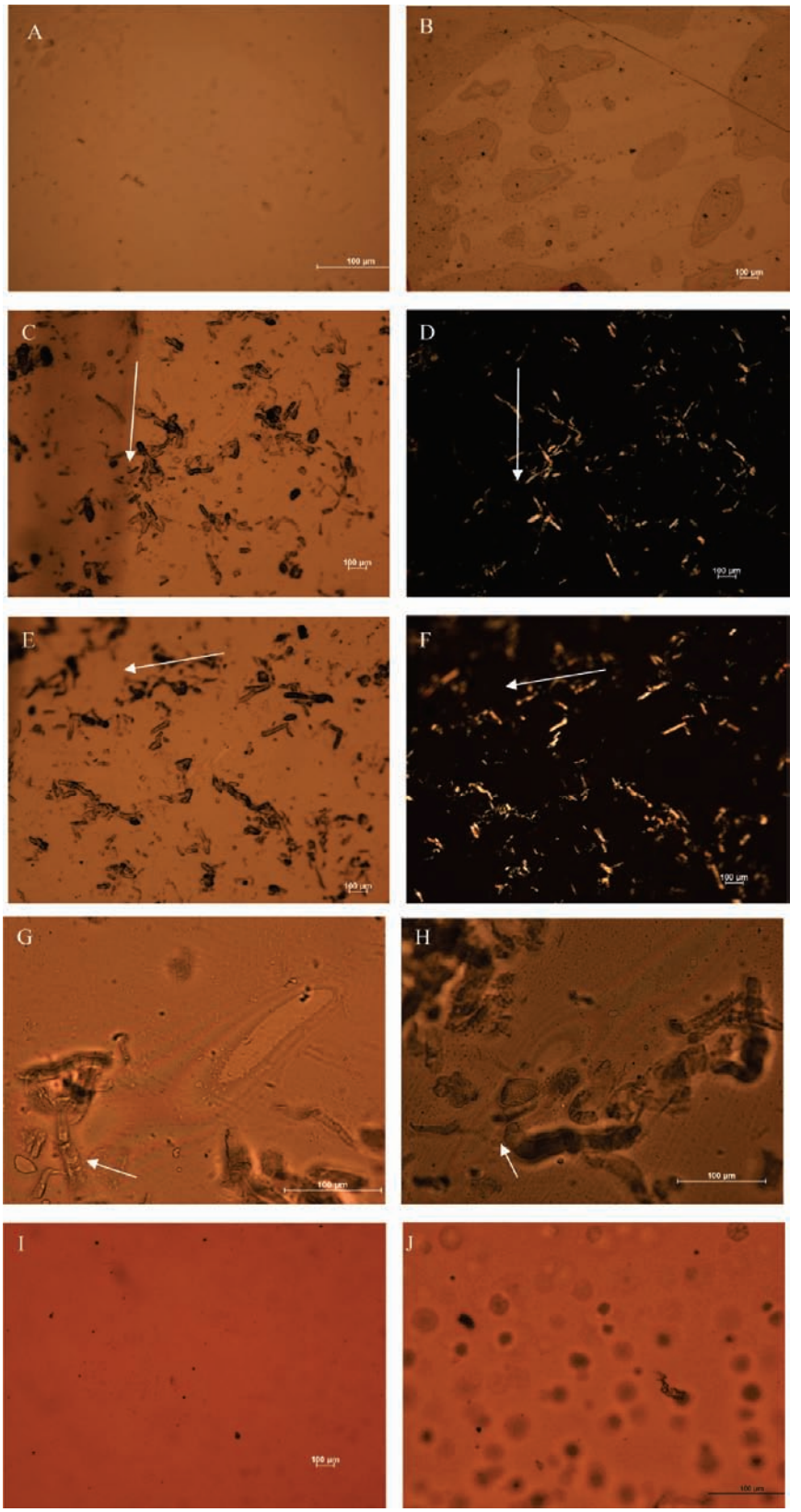


**Figure 3.** Optical micrographs of carrageenan-based films containing (**A**) pure carrageenan, (**B**) 10 wt % glycerol, (**C**−**F**) 3 wt % of microfibers and 10 wt % glycerol, (**G**, **H**) 1 wt % of microfibers and 10 wt % glycerol, (**I**) 3 wt % of CNW, and (**J**) 3 wt % of CNW and 10 wt % glycerol. Images **D** and **F** were taken with polarized light. The white arrows indicate glycerol boundaries in the images. The scale markers are 100 $\mu$m in all cases.

the behavior of adding cellulose microfibers to the carrageenan containing glycerol was found to be rather similar to that of CNW.

Previous studies reported that glycerol can help increase dispersion and interaction with fillers and, hence, the higher stability of the blends with glycerol could be ascribed to this phenomenon (*13*, *36*, *37*). Nevertheless, although it is possible that a better interaction can occur in the composites containing glycerol, a better dispersion was in fact not observed in the current

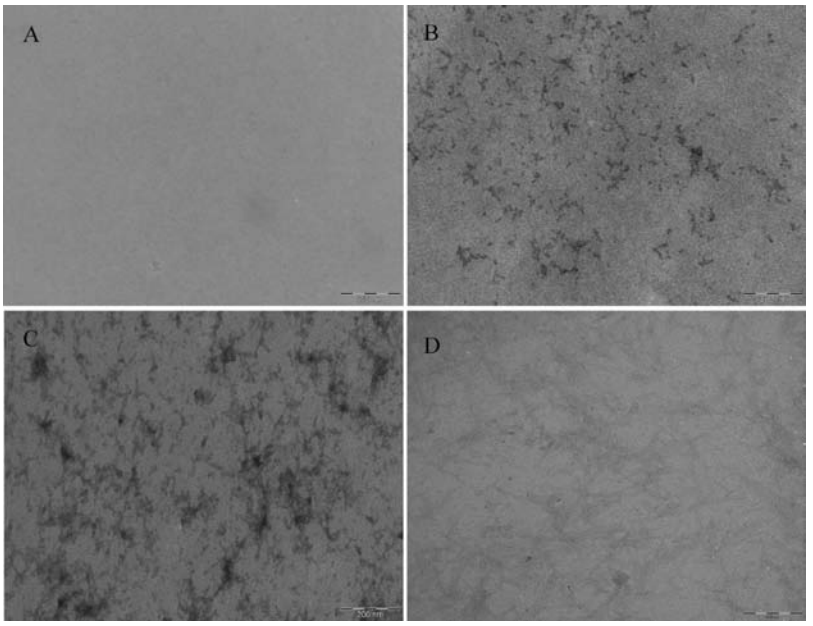


**Figure 4.** TEM images of (**A**) carrageenan film (scale marker is 200 nm), (**B**) carrageenan containing 1 wt % CNW content (scale marker is 200 nm), (**C**) carrageenan containing 5 wt % of CNW (scale marker is 200 nm), and (**D**) cellulose nanowhiskers obtained by direct casting over a TEM grid followed by solvent evaporation (scale marker is 500 nm).

**Table 1.** TGA Maximum of the Weight Loss First Derivative ($T_d$) and the Corresponding Peak Onset and Endset Values for the Carrageenan-Based Materials

| sample | onset (°C) | $T_d$ (°C) | endset (°C) | sample | onset (°C) | $T_d$ (°C) | endset (°C) |
|---|---|---|---|---|---|---|---|
| carrageenan | 211.9 | 219.8 | 226.4 | carrageenan + 10% Gly | 213.2 | 223.3 | 233.0 |
| carrageenan + 1% CNW | 196.8 | 201.9 | 207.0 | carrageenan + 1% CNW + 10% Gly | 221.7 | 227.5 | 233.3 |
| carrageenan + 3% CNW | 204.9 | 210.0 | 215.7 | carrageenan + 3% CNW + 10% Gly | 226.0 | 231.1 | 236.3 |
| carrageenan + 5% CNW | 218.7 | 222.5 | 227.9 | carrageenan + 5% CNW + 10% Gly | 227.0 | 231.7 | 237.2 |
| carrageenan + 1% fiber | 206.9 | 211.7 | 216.9 | carrageenan + 1% fiber + 10% Gly | 211.8 | 227.1 | 233.4 |
| carrageenan + 3% fiber | 191.6 | 196.4 | 201.7 | carrageenan + 3% fiber + 10% Gly | 224.4 | 229.2 | 234.3 |
| carrageenan + 5% fiber[a] | | | | carrageenan + 5% fiber + 10% Gly | 222.4 | 228.1 | 233.3 |
| CNW | 312.6 | 331.5 | 349.0 | CNW | 312.6 | 331.5 | 349.0 |
| purified cellulose microfibers | 309.8 | 363.9 | 384.2 | purified cellulose microfibers | 309.8 | 363.9 | 384.2 |

[a] TGA of carragenan containing 5 wt % of fiber was not measured.

experiments in the cellulose microfibers. This also points out that, in fact, glycerol is a stabilizing agent on its own because it also stabilizes the pure matrix. With regard to the losses in thermal stability for unplasticized nanocomposites with low contents of cellulosic materials, it is feasible that because dispersion is higher at low loadings but the reinforcing effect is higher in terms of water resistance (see later), higher influence in the performance of the composites compared to the matrix could be detrimental to the stability. Therefore, the results here suggest that higher dispersion leads to earlier matrix degradation due to enhanced interaction between filler and matrix and/or the corresponding property alterations.

Overall, the TGA data indicate that the nanobiocomposites are thermally stable in the temperature range in which carrageenan is typically processed, that is, below 190 °C.

**Mass Transport Properties. Table 2** gathers the direct water vapor permeability coefficients of carrageenan and its nanobiocomposites. These values are in good agreement with the values previously reported by the authors in similarly produced films (*4*). From **Table 2**, it can also be seen that a water vapor permeability decrease of ca. 32% is observed with the addition of 10 wt % of glycerol. This is expected as Talja et al. reported that the water vapor permeability for potato starch-based films without plasticizer was higher compared to that of starch-based films plasticized with 20 wt % of glycerol at various RH conditions (*39*). However, as opposed to this, the films plasticized with 30 and 40 wt % of glycerol increased the water vapor permeability (*38*,*39*,). In the current study, a similar behavior of a water vapor permeability reduction at low additions of glycerol was observed in carrageenan films. Visible cracks in the carrageenan film without plasticizer were not seen before testing. However, the increase in water vapor permeability of carrageenan in the absence of glycerol could be hypothesized as being caused by microcracks in the film. Alternatively, Guo et al. reported that cellulose acetate films at plasticizer contents of 5−10% (w/w, solids) had lower water vapor permeability than films without plasticizer because of the decreased molecular mobility of the cellulose acetate promoted by the plasticizer (*40*).

**Figure 5** shows a plot summarizing the water vapor permeability of neat carrageenan and its nanocomposites with CNW and of the corresponding biocomposites with the original cellulose microfibers for various filler contents with and without glycerol. From the results, in the case of the films without glycerol (**Figure 5A**), reductions of water vapor permeability of ca. 68, 70, and 58% were obtained in films containing 1, 3, and 5 wt % of CNW, respectively, compared with unfilled carrageenan. In the case of the composites of carrageenan with the original microfibers, decreases in water vapor permeability of ca. 40, 56, and 8% with the addition of 1, 3, and 5 wt % of microfibers compared to neat carrageenan were obtained. Thus, at higher microfiber contents,

**Table 2.** Water Vapor Permeability for the Carrageenan-Based Materials[a]

| sample | $P$ (kg m/s m$^2$ Pa) | % reduction | sample | $P$ (kg m/s m$^2$ Pa) | % reduction |
|---|---|---|---|---|---|
| carrageenan | $^{AB}6.86 \pm 0.041E^{-14}$ | | carrageenan + 10% Gly | $^{ABC}4.65 \pm 0.542E^{-14}$ | |
| carrageenan + 1% CNW | $^{C}2.16 \pm 0.23E^{-14}$ | **68** | carrageenan + 1% CNW + 10% Gly | $^{C}2.32 \pm 0.15E^{-14}$ | 50 |
| carrageenan + 3% CNW | $^{C}2.01 \pm 0.37E^{-14}$ | **71** | carrageenan + 3% CNW + 10% Gly | $^{C}1.87 \pm 0.14E^{-14}$ | 60 |
| carrageenan + 5% CNW | $^{BC}2.89 \pm 0.57E^{-14}$ | **58** | carrageenan + 5% CNW + 10% Gly | $^{C}1.74 \pm 0.78E^{-14}$ | 63 |
| carrageenan + 1% fiber | $^{AB}4.15 \pm 0.12E^{-14}$ | 40 | carrageenan + 1% fiber + 10% Gly | $^{ABC}4.62 \pm 0.53E^{-14}$ | |
| carrageenan + 3% fiber | $^{BC}3.00 \pm 0.69E^{-14}$ | 56 | carrageenan + 3% fiber + 10% Gly | $^{A}7.11 \pm 1.52E^{-14}$ | |
| carrageenan + 5% fiber | $^{AB}6.31 \pm 0.54E^{-14}$ | 8 | carrageenan + 5% fiber + 10% Gly | $^{A}7.32 \pm 0.51E^{-14}$ | |
| [4,38]*κ*/*ι*-carrageenan literature value | $6.7E^{-14}$ | | | | |

[a] Statistical analysis by Tukey test is indicated by A, B, and C.

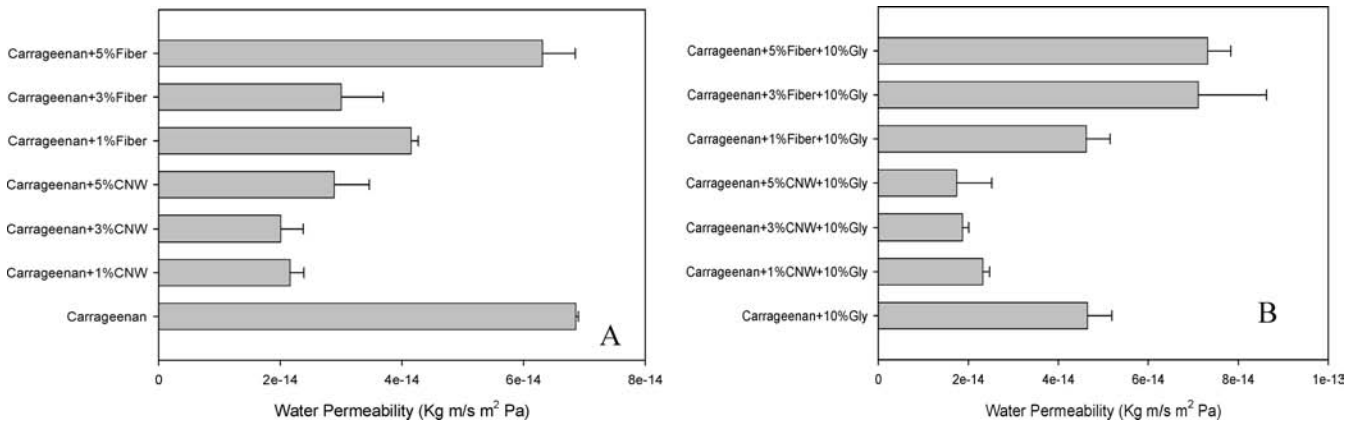


**Figure 5.** (**A**) Permeability to water of carrageenan and its nanocomposites containing 1, 3, and 5 wt % of CNW and of cellulose microfibers. (**B**) Permeability to water of carrageenan with 10 wt % of glycerol and of its nanocomposites containing 1, 3, and 5 wt % of CNW and of cellulose microfibers.

the water vapor permeability reduction is most likely decreased due to filler agglomeration as observed by optical microscopy (see **Figure 1E**). This result is consistent with a previous study on the addition of similar cellulose microfibers to PLA, in which filler agglomeration as observed by SEM occurred with increasing filler loading and resulted in increased permeability due to the creation of preferential paths for diffusion (*32*). Interestingly, for similar filler contents, the CNW are more efficient in reducing water vapor permeability compared to the microfibers due to chiefly nanodispersion versus microdispersion of the filler.

When nanocomposites with glycerol were formulated, a reduction in water vapor permeability was also observed (see **Table 2** and **Figure 5B**); that is, reductions of ca. 50, 60, and 63% were obtained for 1, 3, and 5 wt % of nanofiller contents, respectively, with regard to the matrix containing glycerol. In principle, the barrier reinforcement was not seen higher than for the samples without glycerol, a fact that perhaps rules out the hypothesis of higher dispersion between the filler and the matrix assisted by glycerol. This may also suggest that the observation of glycerol increasing the thermal stability of the blend may be regarded as the plasticizer increasing interaction between the filler and the matrix and/or acting as a stabilizer during the thermal runs. The facts that the glycerol is not miscible with the carrageenan (*31*) and that the cellulosic material may not be as well dispersed in the glycerol phase can lead to a more unhomogeneous dispersion of the nanofiller in the glycerol-containing composites, which in turn can promote higher overall thermal stability for the blends. In sharp contrast to the behavior of the CNW, the addition of 1 wt % of microfibers did not result in enhanced barrier performance, and but adding 3 and 5 wt % of the original microfibers increased water vapor permeability by ca. 53 and 57% compared to pure carrageenan containing glycerol. This behavior in barrier performance is unexpected here but was already reported before in PLA (*32*); cellulose microfiber loadings beyond 1 wt % resulted in barrier deterioration due to sudden microfiber agglomeration and lack of adhesion at the polymer−filler interphase as characterized by SEM. In the current experiments, if the microfiller was not homogeneously dispersed but rather segregated to the matrix phase as the morphology study suggested, this could detrimentally affect the barrier performance. It is also relevant to point out that higher thermal stability seems to be actually promoted in the current experiments by filler agglomeration.

In summary, the best water barrier performance was found for CNW loadings of ca. 3 wt %. This suggests that higher CNW contents lead to nanofiller agglomerations that no longer enhance dispersion and which are detrimental in terms of barrier enhancement. Surprisingly, microfibers become inefficient as barrier elements in the presence of glycerol, due to most likely segregation and agglomeration of the microfibers outside glycerol domains.

To better assess the barrier performance, some typical models were applied to compare the experimental results with widely used simple models. Nielsen (*41*) developed an expression to model the permeability of a two-phase composite sheet in which impermeable square plates are dispersed in a continuous conducting matrix. The plates are oriented so that the two edges of equal length, $L$, are perpendicular to the direction of transport and the third edge, of width $W$, is parallel to the direction of transport. This expression is

$$P = P_m(1-\phi_d)/[1+(L/2W)\phi_d] \quad (1)$$

where $P$ is the permeability of the composite, $P_m$ is the permeability of the matrix, and $\Phi_d$ is the volume fraction of the impermeable filler. The $(1 - \Phi_d)$ term accounts for volume exclusion and the $(1 + (L/2W)\Phi_d)$ term for tortuosity. In the following, this model will be called the tortuosity model. Note that this model does not account for permeation through the dispersed phase.

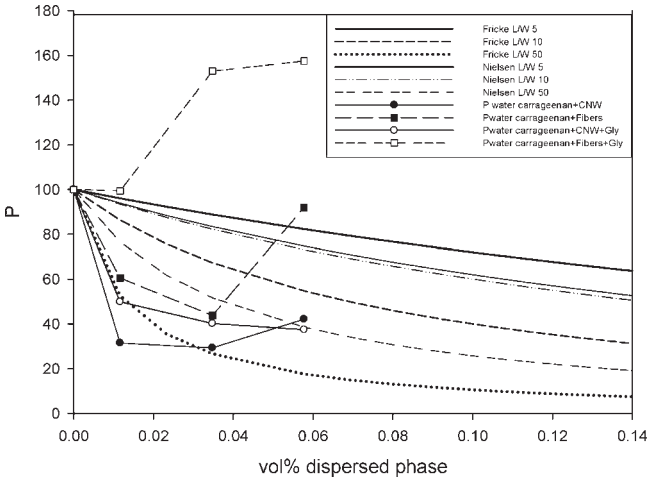


**Figure 6.** Permeability modeling versus volume percent of a dispersed phase with different aspect ratios $L/W$ and the normalized experimental permeability values.

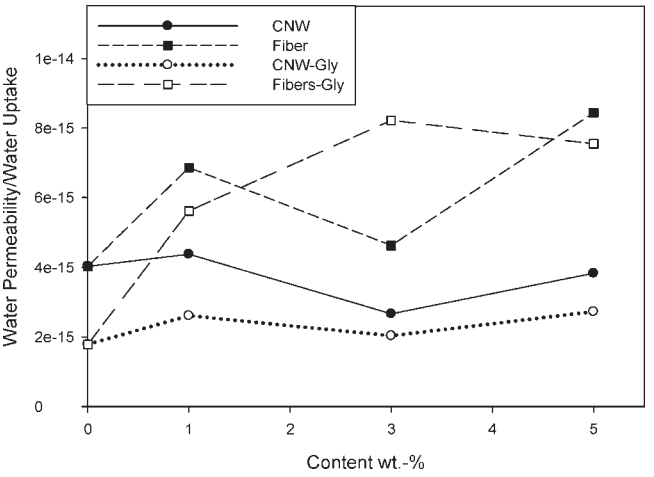


**Figure 7.** Water vapor permeability/percent water uptake ratio at 75% RH for the various samples with and without glycerol.

A more realistic system to consider is one in which a discontinuous low-permeability phase is present in a high-permeability matrix. Maxwell (*42*) developed a model to describe the conductivity of a two-phase system in which permeable spheres are dispersed in a continuous permeable matrix. Fricke (*43*) extended Maxwell's model to describe the conductivity of a two-phase system in which ellipsoids with permeability $P_d$ are dispersed in a more permeable continuous matrix. According to this model, the permeability of the composite system with $\Phi_2$, the volume fraction of the dispersed phase, is (*44*)

$$P = (P_m + P_d F)/(1 + F) \quad (2)$$

where

$$F = [\phi_2/1 - \phi_2][1/(1 + (1 - M)(P_d/P_m - 1))]$$

$$M = \cos\theta/\sin^3\theta[\theta - {}^1/_2 \sin 2\theta]$$

and

$$\cos\theta = W/L$$

$W$ is the dimension of the axis of the ellipsoid parallel to and $L$ the dimension perpendicular to the direction of transport, and $\theta$ is in radians.

**Figure 6** plots the experimental permeability values and modeling results using eqs 1 and 2. TEM characterization of CNW in the carrageenan films suggested experimental $L/W$ (particle length/width ratio) values ranging from 5 to 10 and in the cellulose microfibers from 2 to 15. Therefore, in fact, the main relevant factor in reducing permeability in these models for a given filler loading is to have higher $L/W$ for the filler. Curiously enough, the $L/W$ factors achieved as a result of the top−bottom nanofabrication approach do not change to a significant extent and, hence, the two models for a start cannot really pick up the overall downsizing differentiating effect. Another factor not involved in the modeling is the different permeability blocking capacity for a given filler loading, which for the case of the CNW is hypothesized to be higher because the overall crystallinity of the filler is increased during nanofabrication.

The following set of parameters were used in eqs 1 and 2: $\rho_{\text{cellulose nanowhiskers}} = 1.6$ g/mL (*45*), $P_d \approx 0$, $P_m = 100$, and $L/W$ of 5, 10, and 50. The results displayed in **Figure 7** suggest that the permeability drop in nanobiocomposites containing 1 and 3 wt % of CNW does not follow the expected trend in permeability drop (that is, they arrest earlier) and is actually much higher than predicted for aspect ratios between 5 and 10. However, for aspect ratios of 50, which seem larger than the actual experimental aspect ratios, a better fit to the experimental data is achieved (see **Figure 6**), especially at both 1 wt % of CNW with glycerol and of microfibers without glycerol. It is also observed that the Fricke model better describes the experimental data at low contents of CNW when considering $L/W = 50$. This indicates that a nanodispersion factor should be implemented in the modeling when the filler does not change the $L/W$ ratio to account for overall size reduction. Data for the carrageenan film with 5 wt % of CNW, as the filler seems to more strongly agglomerate, deviate from the modeling expected trend as filler content builds up. This again suggests that filler agglomeration has to be taken into account in the modeling as it reduces the expected barrier enhancement. In the case of the films with cellulose microfibers and glycerol, the water vapor permeability was seen to increase and shows a completely different behavior from the model predictions. We conjecture that the agglomerated morphology of the cellulose microfibers in the carrageenan films and the lack of homogeneity in dispersion could be at the origin of the discrepancy between experimental data for cellulose microfibers and the models.

Nevertheless, the applied simple models largely underpin their barrier responses on the bases of the so-called morphological tortuosity effect at low filler loadings, which is mostly related to diffusion, so they conjecture that a diffusion reduction by a filler-assisted blocking of the permeants is the chief phenomenon accounting for the permeability reductions. To gain more knowledge in this respect, evaluation of water solubility by measuring water uptake was also carried out in the samples.

**Water Uptake. Table 3** summarizes the water uptake at 11, 54, and 75% RH in carrageenan with and without glycerol and in the nanobiocomposites with CNW and cellulose microfibers. A general observation is that water uptake in all films increased with increasing RH, as expected (*39*). However, for the case of the microfiber-based composites, this increase in water uptake is smaller in the low- and medium-humidity range. In **Table 3**, the water uptake at 11% RH is surprisingly reduced by as much as 77, 91, and 91% with the addition of 1, 3, and 5 wt % of CNW, respectively. At higher relative humidity, namely, at 54 and 75% RH, a similar strong reduction in water uptake is observed as CNW are added to the carrageenan matrix. In the case of the

**Table 3.** Percent Water Uptake at 11, 54, and 75% Relative Humidity (RH) for the Carrageenan-Based Materials[a]

| | water uptake at 11% RH | water uptake at 54% RH | water uptake at 75% RH |
|---|---|---|---|
| carrageenan | $^{AB}5.12 \pm 0.08$ | $^{A}10.90 \pm 0.29$ | $^{B}17.02 \pm 0.34$ |
| carrageenan + 1 wt % CNW | $^{DE}1.18 \pm 0.01$ | $^{D}3.49 \pm 0.52$ | $^{C}4.93 \pm 1.29$ |
| carrageenan + 3 wt % CNW | $^{E}0.45 \pm 0.28$ | $^{CD}4.20 \pm 0.19$ | $^{C}7.54 \pm 0.45$ |
| carrageenan + 5 wt % CNW | $^{E}0.41 \pm 0.09$ | $^{CD}4.18 \pm 0.19$ | $^{A}7.54 \pm 0.38$ |
| carrageenan + 10% Gly | $^{ABCDE}3.62 \pm 0.32$ | $^{A}12.41 \pm 0.21$ | $^{C}6.03 \pm 0.62$ |
| carrageenan + 1 wt % CNW + 10% Gly | $^{CDE}1.46 \pm 0.04$ | $^{BC}6.13 \pm 0.012$ | $^{C}8.89 \pm 0.62$ |
| carrageenan + 3 wt % CNW + 10% Gly | $^{E}0.85 \pm 0.10$ | $^{CD}4.77 \pm 0.39$ | $^{BC}9.19 \pm 2.38$ |
| carrageenan + 5 wt % CNW + 10% Gly | $^{A}1.93 \pm 0.89$ | $^{BCD}5.05 \pm 0.93$ | $^{C}6.38 \pm 0.84$ |
| carrageenan + 1 wt % fiber | $^{ABCD}4.71 \pm 0.25$ | $^{CD}4.57 \pm 0.28$ | $^{C}6.05 \pm 0.57$ |
| carrageenan + 3 wt % fiber | $^{ABC}4.74 \pm 0.42$ | $^{BCD}5.24 \pm 0.15$ | $^{C}6.49 \pm 0.02$ |
| carrageenan + 5 wt % fiber | $^{AB}5.19 \pm 0.07$ | $^{BCD}5.31 \pm 0.44$ | $^{C}7.48 \pm 0.82$ |
| carrageenan + 1 wt % fiber + 10% Gly | $^{A}5.87 \pm 0.50$ | $^{BC}5.87 \pm 0.10$ | $^{C}8.23 \pm 2.13$ |
| carrageenan + 3 wt % fiber + 10% Gly | $^{A}5.61 \pm 1.85$ | $^{B}6.97 \pm 0.05$ | $^{C}8.65 \pm 0.80$ |
| carrageenan + 5 wt % fiber + 10% Gly | $^{AB}5.45 \pm 0.35$ | $^{BC}6.23 \pm 0.08$ | $^{C}9.70 \pm 1.88$ |

[a] Statistical analysis by Tukey test is indicated by A, B, C, D, and E.

composites with fibers, the water uptake at 11% RH shows a similar uptake value as for the pure carrageenan, but at 54 and 75% RH the water uptake is clearly smaller than in carrageenan and rather similar to that in the corresponding CNW-based composites. Thus, the good morphology and dispersion of the highly crystalline CNW (as determined and reported elsewhere (*31*)) in the carrageenan films produced this significant reduction in water uptake. The microfibers also reduce to a significant extent the water uptake but only at medium-high relative humidity conditions.

The impact of adding glycerol to the carrageenan films on water uptake was also determined at different humidity levels. The water uptake of pure carrageenan was seen to decrease with the addition of glycerol at low relative humidity, but increased at higher relative humidity. The same behavior was reported by Zeppa et al. (*46*). Thus, glycerol was also reported to decrease water uptake at low water activity and to increase this at high water activity. In particular, at low water activity, the decrease in solvent uptake was attributed to a decrease of available sorption sites in the presence of the plasticizer. The rationale for this is that in plasticized films there are interactions between the hydroxyl groups of the polysaccharide and these of glycerol, and so there are fewer sorption sites for water binding (*39*, *46*). When CNW are added, the available free volume is also thought to be filled in by the highly crystalline nanofiller, hence resulting in reduced uptakes. That effect seems less efficient with microfibers at low water activity. At medium-high relative humidity conditions, water-clustering phenomena resulting in plasticization are thought to occur, thus increasing the overall water uptake as observed here (*46*). This phenomenon is thought to be more favored in the glycerol plasticized films due to enhanced molecular mobility of the polymer chains in the presence of the plasticizer and also to the hydrophilicity of the plasticizer.

**Table 3** also shows that films of carrageenan with 10 wt % of glycerol and with 1, 3, and 5 wt % of CNW present a decrease in the water uptake at 11% RH of ca. 60, 76, and 47%, respectively, compared with the plasticized carrageenan containing glycerol. In the case of the water uptake at 54% RH, reductions of 50, 61, and 59% were observed for the films of carrageenan with 1, 3, and 5 wt % of CNW. Water uptakes measured at 75% RH were also seen to present decreases of ca. 66, 65, and 75% for the glycerol plasticized films containing 1, 3, and 5 wt % of CNW. At low and medium water activity, the water uptake reductions are clearly smaller in the presence of glycerol than in the absence of the plasticizer. In the case of the composites of carrageenan with cellulose microfibers, an increase in water uptake at 11% RH was seen. On the other hand, at higher humidity conditions, the microfibers exhibit significantly reduced water uptake, which becomes similar as this observed for the CNW. The behavior in water uptake at low humidity conditions does single out the behavior of the microcomposites containing glycerol, but curiously this is not the case at high humidity and, therefore, the reproducible barrier performance of the microcomposites in the presence of glycerol must be related to diffusion.

As expected, the addition of cellulose nanowhiskers was generally seen to be more efficient in reducing water sorption across relative humidity in the presence and in the absence of glycerol due to both the higher crystallinity present in the CNW and the higher dispersion in the matrix due to the nanosize. Interestingly, the exhibited water uptake drops are generally similar to the corresponding water vapor permeability reductions and, hence, a surprisingly strong contribution to permeability is anticipated from this solubility indicative factor.

To further study the impact of solubility or water uptake on the observed permeability, **Figure 7** shows the ratio of water vapor permeability measured at 75% RH divided by water uptake at 75% RH for the carrageenan films and the nanocomposites containing CNW and cellulose microfibers with and without glycerol. This ratio can tell us something about the water diffusion ($D = P/S$) in the materials at this high relative humidity condition. From the results, it is surprising to see that in fact diffusion seems to be rather constant or to decrease in unplasticized CNW based-biocomposites and to slightly increase in plasticized CNW based-composites, suggesting that the water solubility reduction is a strong factor behind the reduction in moisture permeability in the nanobiocomposites. A higher water diffusion seems clearer in the microcomposites and especially for the samples containing glycerol, a fact that again supports the lower dispersion and/or interfacial interaction and agglomeration of the microfiller in the glycerol-containing samples. These observations are very relevant because they may provide a better understanding of the barrier effect of the CNW as based on the presence of crystalline blocks, which reduce solubility to a significant extent and, hence, permeability.

**Conclusions.** As a summary, cellulose nanowhiskers, with lengths ranging from 25 to 50 nm and cross sections around 5 nm, were prepared from highly purified α-cellulose microfibers (of 50−100 $\mu$m length and 10−20 $\mu$m cross section) by acid hydrolysis and were used to reinforce the water barrier of a carrageenan matrix with contents ranging from 1 to 5 wt % using a solvent casting method. From TGA results, the addition of low contents of nanowhiskers in the carrageenan films was seen to

reduce to some extent the overall thermal stability of the biopolymer, which was reversed by filler agglomeration at higher loadings and with the addition of the plasticizer glycerol. Addition of cellulose nanowhiskers to carrageenan resulted in good dispersion of the nanofiller in the matrix, especially at low filler contents. However, increasing the nanofiller loading in excess of 3 wt % TEM and water vapor permeability data suggested that agglomeration of these CNW takes place due to hydrogen-bonding-induced self-association. Optimum performance in terms of barrier, that is, a ca. 70% water vapor permeability drop, was seen to occur at around 3 wt % of CNW. The permeability drop was chiefly ascribed to a strong reduction in water uptake rather than a diffusion-driven tortuosity effect. On the other hand, the addition of the parent cellulose microfibers did also result in reductions in permeability at low filler loadings, but these were smaller per filler volume compared to the CNW and were seen only in the absence of the plasticizer glycerol. The optical properties of the microcomposites were detrimentally affected compared to both CNW-based composites and pure carrageenan. Surprisingly, the addition of glycerol resulted in increased permeability for the microcomposites due to most likely segregation of the cellulosic material to the matrix fraction as suggested by optical microscopy and subsequent agglomeration and creation of preferential paths for diffusion.

Overall, the main conclusion arising from this study is that cellulose nanowhiskers obtained by acid hydrolysis can be used to enhance the water barrier and resistance of carrageenan and hence can have significant potential in food-packaging and -coating applications.

## ACKNOWLEDGMENT5

The authors would like to thank the MICINN projects MAT2009-14533-C02-01, EUI2008-00182, the projects POCTI/EQU/45595/2002 and POCI/EQU/58064/2004 and the EU FP7 project EcoBioCap for financial support. Finally, M.DSG would like to thank the FPI program of the GV associated to the MEC project MAT2003-08480-C3 for the research grant.

## LITERATURE CITED

(1) Hilliou, L.; Larotonda, F. D. S.; Abreu, P.; Ramos, A. M.; Sereno, A. M.; Gonçalves, M. P. Effect of extraction parameters on the chemical structure and gel properties of $\kappa/\iota$-hybrid carrageenans obtained from *Mastocarpus stellatus*. *Biomol. Eng.* **2006**, *23*, 201−208.

(2) Hilliou, L.; Larotonda, F. D. S.; Sereno, A. M.; Gonçalves, M. P. Thermal and viscoelastic properties of $\kappa/\iota$-hybrid carrageenan gels obtained from the Portuguese seaweed *Mastocarpus stellatus*. *J. Agric. Food Chem.* **2006**, *54* (20), 7870−7878.

(3) Hilliou, L.; Gonçalves, M. P. Gelling properties of a $\kappa/\iota$-hybrid carrageenan: effect of concentration and steady shear. *Int. J. Food Sci. Technol.* **2007**, *42*, 678−685.

(4) Larotonda, F. D. S.; Hilliou, L.; Goncalves, M. P.; Sereno, A. M. From low value renewable resources to green biomaterials for edible coating applications. In *Recent Advances in Research on Biodegradable Polymers and Sustainable Composites*; Jiménez, A., Zaikoz, G. E., Eds.; 2008; Nova Science: Hauppauge, NY, Vol. 3, Chapter 19, ISBN 978-1-60692-155-5.

(5) De Ruiter, G. A.; Rudolph, B. Carrageenan biotechnology. *Trends Food Sci. Technol.* **1997**, *8*, 389−395.

(6) Shaw, C.; Secrist, J.; Tuomy, J. Method of extending the storage life in the frozen state of precooked foods and product produced. U.S. Patent 4,196,219, 1980

(7) Macquarrie, R. Edible film formulation. U.S. Patent 0155200 A1, 2002.

(8) Ninomiya, H.; Suzuki, S.; Ishii, K. Edible film and method of making same. U.S. Patent 5,620,757, 1997

(9) Tanner, K.; Getz, J.; Burnett, S.; Youngblood, E.; Draper, P. Film forming compositions comprising modified starches and iota-carrageenan and methods for manufacturing soft capsules using same. U.S. Patent 0081331 A1, 2002.

(10) Bartkowiak, A.; Hunkeler, D. Carrageenan−oligochitosan microcapsules: optimization of the formation process. *Colloids Surf. B: Biointerfaces* **2001**, *21*, 285−298.

(11) Fonkwe, L.; Archibald, D.; Gennadios, A. Nongelatin capsule shell formulation. U.S. Patent 0138482 A1, 2003

(12) Brody, A. L. Edible packaging. *Food Technol.* **2005**, *59*, 65.

(13) Sanchez-Garcia, M. D. Hilliou, L. Lagaron, J. M. Nanobiocomposites of carrageenan, zein and mica of interest in food packaging and coating applications. *J. Agric. Food Chem.* **2010**, *58*, 6884−6894.

(14) Sturcova, A.; Davies, G. R.; Eichhorn, S. J. The elastic modulus and stress-transfer properties of tunicate cellulose whiskers. *Biomacromolecules* **2005**, *6*, 1055−1061.

(15) Podsiadlo, P.; Choi, S.; Shim, B.; Lee, J.; Cussihy, M.; Kotov, N. *Biomacromolecules* **2005**, *6*, 2914−2918.

(16) Azizi Samir, M. A. S.; Alloin, F.; Dufresne, A. A review of recent research into cellulosic whiskers, their properties and their application in nanocomposite field. *Biomacromolecules* **2005**, *6*, 612−626.

(17) Marchessault, R. H.; Morehead, F. F.; Walter, N. M. Liquid crystal systems from fibrillar polysaccharides. *Nature* **1959**, *184*, 632−633.

(18) Dufresne, A.; Kellerhals, M. B.; Witholt, B. Transcrystallization in Mcl-PHAs/cellulose whiskers composites. *Macromolecules* **1999**, *32*, 7396−7401.

(19) López-Suevos, F.; Eyholzer, C.; Bordeanu, N.; Richter, K. DMA analysis and wood bonding of PVAc latex reinforced with cellulose nanofibrils. *Cellulose* **2010**, *17* (2), 387−398.

(20) Dufresne, A.; Cavaille, J. Y.; Helbert, W. Thermoplastic nanocomposites filled with wheat straw cellulose whiskers. Part II: Effect of processing and modeling. *Polym. Compos.* **1997**, *18*, 198.

(21) Chen, Y.; Liu, C.; Chang, P. R.; Cao, X.; Anderson, D. P. Bionanocomposites based on pea starch and cellulose nanowhiskers hydrolyzed from pea hull fibre: effect of hydrolysis time. *Carbohydr. Polym.* **2009**, *76*, 607−615.

(22) Kvien, I.; Sugiyama, J.; Votrubec, M.; Oksman, K. Characterization of starch based nanocomposites. *J. Mater. Sci.* **2007**, *42*, 8163−8171.

(23) Samir, M.; Alloin, F.; Sanchez, J. Y.; Dufresne, A. Cellulose nanocrystals reinforced poly(oxyethylene). *Polymer* **2004**, *45*, 4149.

(24) Samir, M.; Mateos, A. M.; Alloin, F; Sanchez, J. Y.; Dufresne, A. Plasticized nanocomposite polymer electrolytes based on poly(oxyethylene) and cellulose whiskers. *Electrochim. Acta* **2004**, *49*, 4667.

(25) Qian, L.; Jinping, Z.; Lina, Z. Structure and Properties of the Nanocomposite Films of Chitosan Reinforced with Cellulose Whiskers. *J. Polym. Sci.: Part B: Polym. Phys.* **2009**, *47*, 1069−1077.

(26) Wang, Y.; Cao, X.; Zhang, L. Effects of cellulose whiskers on properties of soy protein thermoplastics. *Macromol. Biosci.* **2006**, *6*, 524−531.

(27) Daniel-Da-Silva, A. L.; Lopes, A. B.; Gil, A. M.; Correia, R. N. Synthesis and characterization of porous $\kappa$-carrageenan/calcium phosphate nanocomposite scaffolds. *J. Mater. Sci.* **2007**, *42*, 8581−8591.

(28) Gan, S.-L.; Feng, Q.-L. Preparation and characterization of a new injectable bone substitute-carrageenan/nano-hydroxyapatite/collagen. *Acta Acad. Med. Sin.* **2006**, *28* (5), 710−71.

(29) Hilliou, L.; Larotonda, F. D. S.; Abreu, P.; Ramos, A. M.; Sereno, A. M.; Gonçalves, M. P. Effect of extraction parameters on the chemical structure and gel properties of $\kappa/\iota$-hybrid carrageenans obtained from *Mastocarpus stellatus*. *Biomol. Eng.* **2006**, *23*, 201−208.

(30) Petersson, L.; Kvien, I.; Oksman, K. Structure and thermal properties of poly(lactic acid)/cellulose whiskers nanocomposite materials. *Compos. Sci. Technol.* **2007**, *67*, 2535−2544.

(31) Sanchez-Garcia, M. D.; Lagaron, J. M. On the use of plant cellulose nanowhiskers to enhance the barrier properties of polylactic acid. *Cellulose* **2010**, *17* (5), 987−1004.

(32) Sanchez-Garcia, M. D.; Gimenez, E.; Lagaron, J. M. Mophology and barrier properties of solvent cast composites of thermoplastic biopolymers and purified cellulose fibers. *Carbohydr. Polym.* **2008**, *71*, 235−244.

(33) Oh, S. Y.; Yoo, D. I.; Shin, Y.; Kim, H. C.; Kim, H. Y.; Chung, Y. S.; Park, W. H.; Youk, J. H. Crystalline structure analysis of cellulose

treated with sodium hydroxide and carbon dioxide by means of X-ray diffraction and FTIR spectroscopy. *Carbohydr. Res.* **2005**, *340*, 2376−2391.
(34) Pandey, J. K.; Chu, W. S.; Kim, C. S.; Lee, C. S.; Ahn, S. H. Bio-nano reinforcement of environmentally degradable polymer matrix by cellulose whiskers from grass. *Composites: Part B* **2009**, *40*, 676−680.
(35) Chen, Y.; Liu, C.; Chang, P. R.; Cao, X.; Anderson, D. P. Bionanocomposites based on pea starch and cellulose nanowhiskers hydrolyzed from pea hull fibre: effect of hydrolysis time. *Carbohydr. Polym.* **2009**, *76*, 607−615.
(36) Ayuk, J. E.; Mathew, A. P.; Oksman, K. The effect of plasticizer and cellulose nanowhisker content on the dispersion and properties of cellulose acetate butyrate nanocomposites. *J. Appl. Polym. Sci.* **2009**, *114*, 2723−2730.
(37) Li, Q.; Zhou, J.; Zhang, L. Structure and properties of the nanocomposite films of chitosan reinforced with cellulose whiskers. *J. Polym. Sci. Part B: Polym. Phys.* **2009**, *47*, 1069−1077.
(38) Larotonda, F. D. S.; Hilliou, L.; Goncalves, M. P.; Sereno, A. M. Film properties of $\kappa/\iota$-hybrid carrageenan natural polymer. Present at the Polymer Processing Society 23rd Annual Meeting.
(39) Talja, R. A.; Helen, H.; Kirsi Jouppila, Y. H. R. Effect of various polyols and polyol contents on physical and mechanical properties of potato starch-based films. *Carbohydr. Polym.* **2007**, *67*, 288−295.
(40) Guo, J. H. Effects of plasticizers on water permeation and mechanical properties of cellulose acetate: antiplasticization in slightly plasticized polymer film. *Drug Dev. Ind. Pharm.* **1993**, *19* (13), 1541−1555.
(41) Nielsen, L. W. *J. Macromol Sci.* **1967**, *Al*, 929.
(42) Maxwell, J. C. *Electricity and Magnetism*, 3rd ed.; Dover: New York, 1891; Vol. 1.
(43) Fricke, H. *Phys. Rev.* **1924**, *24*, 575.
(44) Paul, D. R.; Bucknall, C. B. *Polymer Blends*; 2000; Wiley InterScience: NY, Vol. 2: Performance.
(45) Capadona, J. R.; Shanmuganathan, K.; Trittschuh, S.; Seidel, S.; Rowan, S. J.; Weder, C. Polymer nanocomposites with nanowhiskers isolated from microcrystalline cellulose. *Biomacromolecules* **2009**, *10*, 712−716
(46) Zeppa, C.; Gouanvé, F.; Espuche, E. Effect of a plasticizer on the structure of biodegradable starch/clay nanocomposites: thermal, water-sorption, and oxygen-barrier properties. *J. Appl. Polym. Sci.* **2009**, *112*, 2044−2056.
(47) López-Rubio, A.; Lagaron J. M.; Ankerfors, M.; Lindström, T.; Nordqvist, D.; Mattozzi, A.; Hedenqvist, M. S. *Carbohydr. Polym.* **2007**, *68*, 718−727.
(48) Maren, R.; William, W. Effect of sulfate groups from sulfuric-acid hydrolysis on the thermal degradation behavior of bacterial cellulose. *Biomacromolecules* **2004**, *5*, 1671−1677.

**Received for review July 24, 2010. Revised manuscript received September 24, 2010. Accepted November 2, 2010.**